Electronic Supplementary Material (ESI) for…. This journal is ©

Supporting Information

The mechanochemical Scholl reaction as a versatile synthesis tool for the solvent-free generation of microporous polymers

Annika Krusenbaum,[a] Sven Grätz,[a] Sarah Bimmermann,[a] Stefanie Hutsch,[a] Lars Borchardt[a*]

[a] Anorganische Chemie I, Ruhr-Universität Bochum,
Universitätsstr. 150, 44801 Bochum

Table of Contents

1. Materials

Iron(III) chloride (anhydrous, Alfa Aesar, 98% purity), 1,3,5-Triphenylbenzene (Aldrich, 97 % purity), Tetraphenylmethane (BLDpharm, 97% purity), Tetraphenylethylene (chemPUR, 98% purity), 2,4,6-Triphenyl-1,3,5-Triazine (TCI, >98% purity), Triphenylamine (TCI, >98% purity), 1,3,5-Tris(N-carbazolyl)benzene (Aldrich, >97% purity). All chemicals were purchased as received.

Zirconium oxide milling balls (Type ZY-S) in Ø = 5 mm (average weight of 0.40 g), Ø = 10 mm (average weight of 3.2 g) and Ø = 15 mm (average weight of 11.73 g) were purchased from Sigmund Lindner GmbH. Tungsten carbide milling balls (YG6X, G10 surface) in Ø = 10 mm with an average weight of 7.20 g were purchased from Zhuzhou Good Cemented Carbide Co., Ltd. Tempered steel milling balls (1.4125, AISI 440C) in Ø = 10 mm with an average weight of 4.02 g were purchased from TIS Wälzkörpertechnologie GmbH.

2. Milling parameters

Table S1: Overview over the yield, specific surface area (SSA_{BET}) and the total pore volume (V_{total}) for various polymers obtained by the use of different milling parameters.

Polymer	Monomer	Material	Time (s)	Frequency (Hz/rpm) mill	Liquid Amount (ml)	Temperature (°C)	Yield (%)	SSA_{BET} (m^2/g)	V_{total} (g/cm^3)
PP1	A	ZrO_2 (10 mm)	5	30 MM500	/	RT	> 99	658	0.53
PP2	A	ZrO_2 (10 mm)	1	30 MM500	/	RT	19	87	0.17
PP3	A	ZrO_2 (10 mm)	2	30 MM500	/	RT	51	61	0.09
PP4	A	ZrO_2 (10 mm)	10	30 MM500	/	RT	> 99	348	0.28
PP5	A	ZrO_2 (10 mm)	15	30 MM500	/	RT	> 99	505	0.40
PP6	A	ZrO_2 (10 mm)	30	30 MM500	/	RT	> 99	568	0.61
PP7	A	ZrO_2 (10 mm)	60	30 MM500	/	RT	> 99	421	0.33

PP8	A	ZrO_2 (10 mm)	5	10 MM500	/	RT	26	17	0.06
PP9	A	ZrO_2 (10 mm)	5	20 MM500	/	RT	44	87	0.13
PP10	A	ZrO_2 (10 mm)	5	25 MM500	/	RT	75	111	0.18
PP11	A	ZrO_2 (10 mm)	5	35 MM500	/	RT	> 99	273	0.24
PP12	A	WC (10 mm)	5	30 MM500	/	RT	> 99	581	0.43
PP13	A	Steel (10 mm)	5	30 MM500	/	RT	> 99	499	0.36
PP14	A	ZrO_2 (5 mm)	5	30 MM500	/	RT	83	285	0.12
PP15	A	ZrO_2 (15 mm)	5	30 MM500	/	RT	> 99	457	0.36
PP16	B	ZrO_2 (10 mm)	5	30 MM500	/	RT	12	225	0.24
PP17	C	ZrO_2 (10 mm)	5	30 MM500	/	RT	86	88	0.24
PP18	D	ZrO_2 (10 mm)	5	30 MM500	/	RT	78	n.p.	-
PP19	E	ZrO_2 (10 mm)	5	30 MM500	/	RT	48	161	0.56
PP20	F	ZrO_2 (10 mm)	5	30 MM500	/	RT	> 99	1408	0.95
PP21	A	Steel (10 mm)	5	30 MM500	/	- 50	68	174	0.36
PP22	A	Steel (10 mm)	5	30 MM500	/	- 20	89	195	0.19
PP23	A	Steel (10 mm)	5	30 MM500	/	0	95	359	0.38
PP24	A	Steel (10 mm)	5	30 MM500	/	50	> 99	595	0.53
PP25	A	Steel (10 mm)	5	30 MM500	/	75	> 99	568	0.47
PP26	A	Steel (10 mm)	5	30 MM500	/	100	> 99	657	0.44
PP27	A	Steel (10 mm)	5	30 MM500	/	125	> 99	522	0.41
PP28	A	ZrO_2 (10 mm)	5	800 P7	DCM 0.5 ml	RT	> 99	1069	0.72

PP29	A	ZrO_2 (10 mm)	5	800 P7	DCM 1 ml	RT	97	1090	0.73
PP30	A	ZrO_2 (10 mm)	5	800 P7	DCM 1.5 ml	RT	> 99	914	0.64
PP31	A	ZrO_2 (10 mm)	5	800 P7	DCM 2 ml	RT	> 99	733	0.52
PP32	A	ZrO_2 (10 mm)	60	800 P7	DCM 1 ml	RT	> 99	998	0.68
PP33	A	ZrO_2 (10 mm)	60	800 P7	$CHCl_3$ 1 ml	RT	> 99	845	0.58
PP34	A	ZrO_2 (10 mm)	60	800 P7	CH_2Br_2 1 ml	RT	87	953	0.63
PP35	A	ZrO_2 (10 mm)	60	800 P7	CH_2BrCl 1 ml	RT	> 99	832	0.57
PP36	A	ZrO_2 (10 mm)	60	800 P7	Et_2O 1 ml	RT	90	55	0.01
PP37	A	ZrO_2 (10 mm)	60	800 P7	EtOH 1 ml	RT	> 99	173	0.10
PP38	A	ZrO_2 (10 mm)	60	800 P7	EtOAc 1 ml	RT	> 99	318	0.27
PP39	A	ZrO_2 (10 mm)	60	800 P7	MeCN 1 ml	RT	> 99	72	0.15
PP40	A	ZrO_2 (10 mm)	60	800 P7	MeOH 1 ml	RT	76	22	0.07
PP41	A	ZrO_2 (10 mm)	60	800 P7	Acetone 1 ml	RT	> 99	39	0.05
PP42	A	ZrO_2 (10 mm)	60	800 P7	THF 1 ml	RT	> 99	71	0.09
Post polymer $FeCl_3$	Polymer	ZrO_2 (10 mm)	30	30 MM500	/	RT	> 99	560	0.39
Post polymer NaCl	Polymer	ZrO_2 (10 mm)	30	30 MM500	/	RT	> 99	432	0.43

Table S2: Comparison between the yields, specific surface areas (SSA_{BET}) and total pore volumes (V_{total}) obtained for the standard reaction (Reaction of 1,3,5-Triphenylbenzene; 12 eq. $FeCl_3$, 5 min) in the Fritsch Pulverisette 7 premium line planetary ball mill (P7) at 800 rpm and in the Retsch mixer mill MM500 (MM500) at 30 Hz. For the reactions, different amounts of DCM were added.

	P7			MM500		
	Yield (%)	**SSA_{BET} (m^2/g)**	**V_{total} (cm^3/g)**	**Yield (%)**	**SSA_{BET} (m^2/g)**	**V_{total} (cm^3/g)**
0.5 ml DCM	> 99	1069	0.72	> 99	976	0.72
1 ml DCM	97	1090	0.73	> 99	990	0.69
1.5 ml DCM	> 99	914	0.64	> 99	956	0.67
2 ml DCM	> 99	733	0.52	> 99	740	0.76*

* sample contains large amounts of interparticular space

3. Characterisation

3.1. PP1 (reference system)

Table S3: Elemental analysis of **PP1**.

	C (wt.%)	H (wt.%)	N (wt.%)	S (wt.%)
Calculated	95.02	4.98	-	-
Found	96.87	2.93	-	-

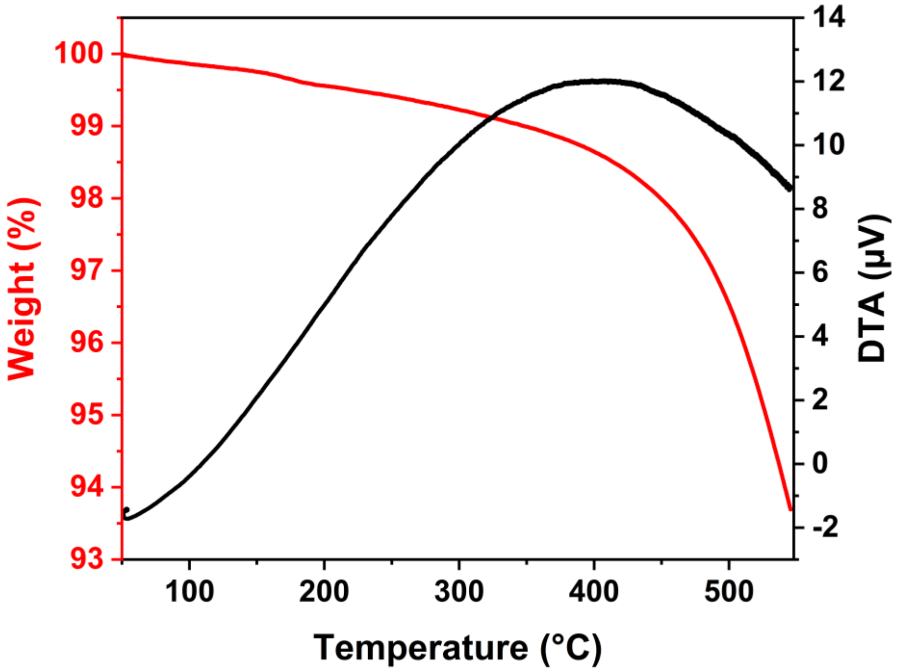

Figure S1: Thermogravimetric analysis (TGA; red) and differential thermal analysis (DTA; black) of the Porous Polymer **PP1**.

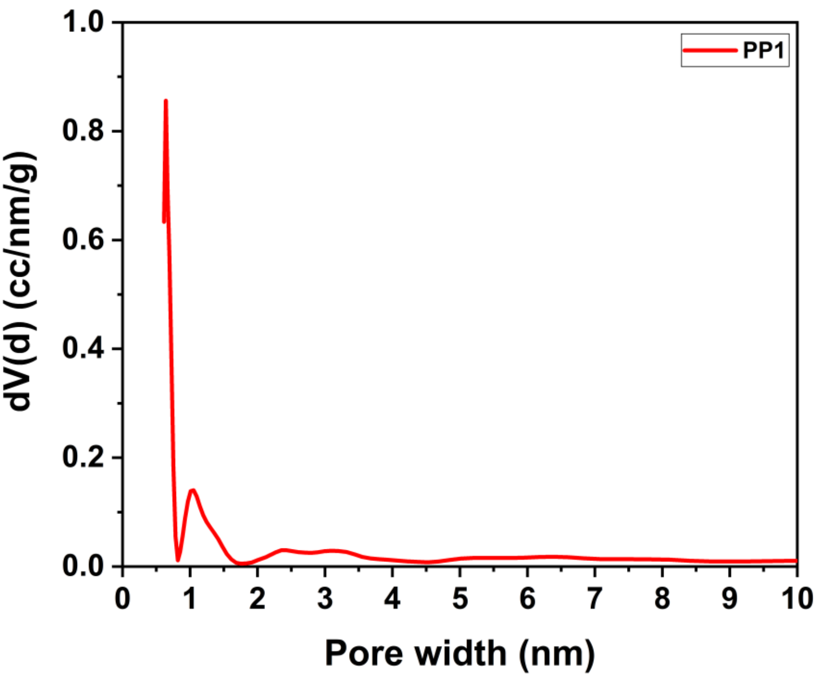

Figure S2: Pore Size distribution (red) of the Porous Polymer **PP1**.

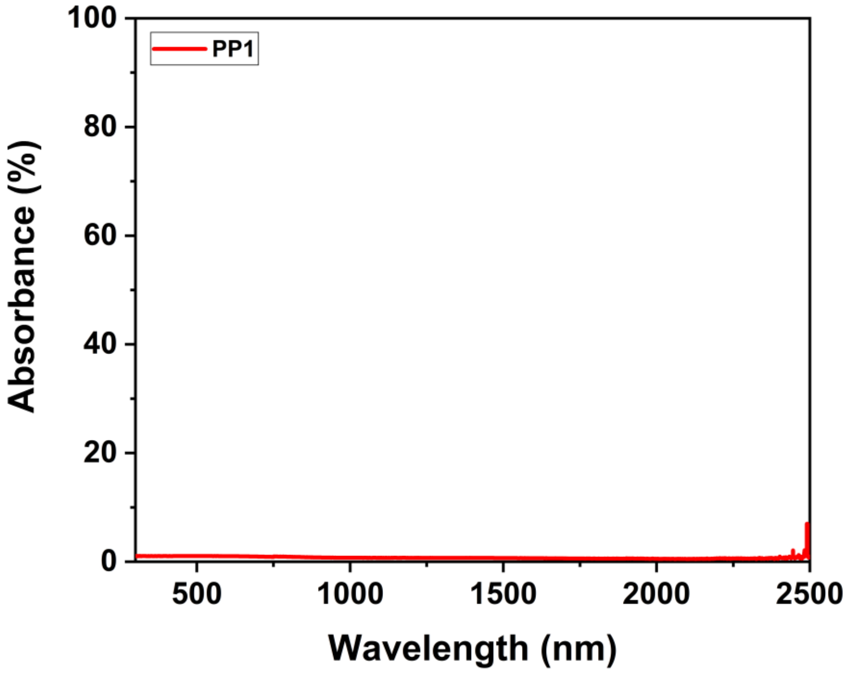

Figure S3: UV/VIS spectrum (red) of the Porous Polymer 1.

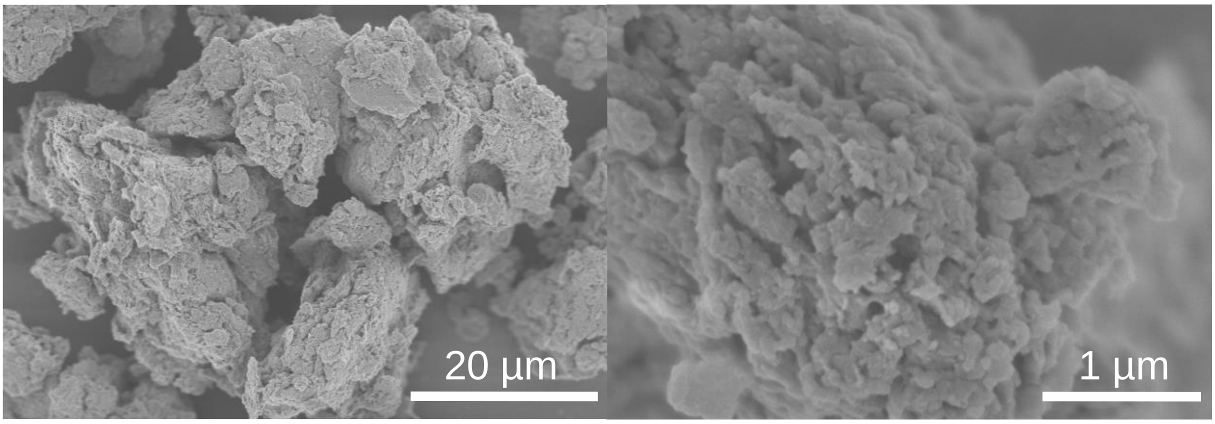

Figure S4: SEM image of the sample **PP1** with a magnitude of 2000 (left) and of 50000 (right).

3.2. PP29 (reference system + 1 ml DCM)

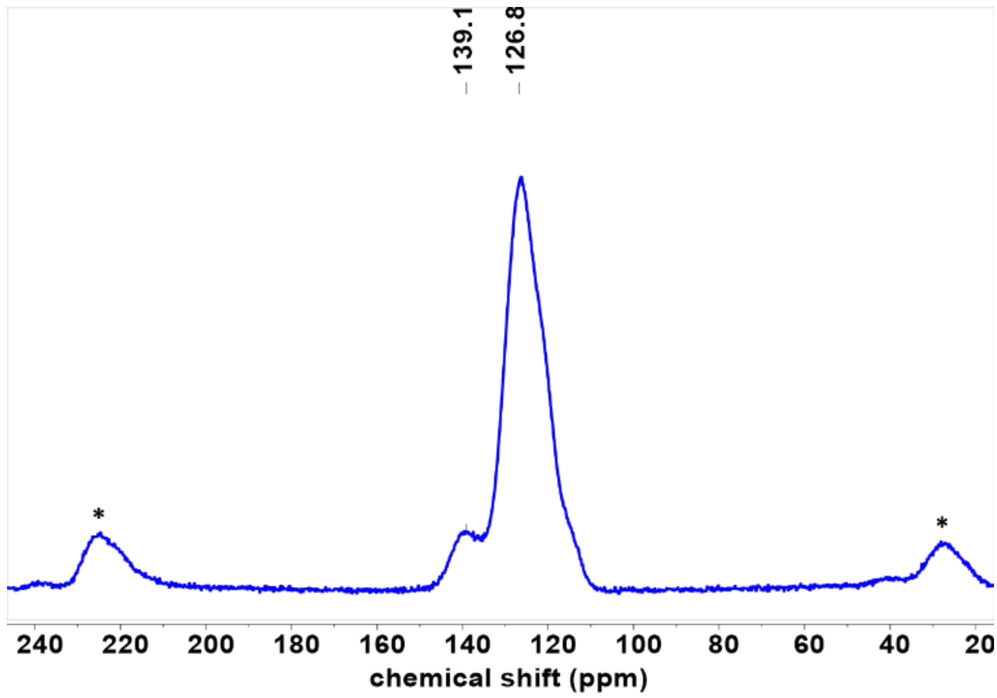

Figure S5: ^{13}C CP-MAS NMR spectrum of **PP29**. The peaks are assigned to the spectrum and the spinning bands are marked with an asterisk.

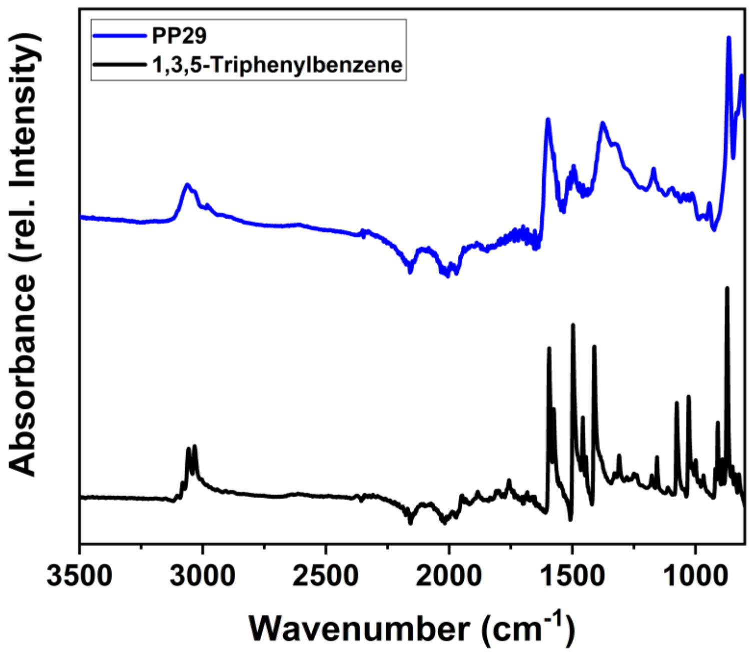

Figure S6: FT-IR spectra of **PP29** (blue) and 1,3,5-Triphenylbenzene (black).

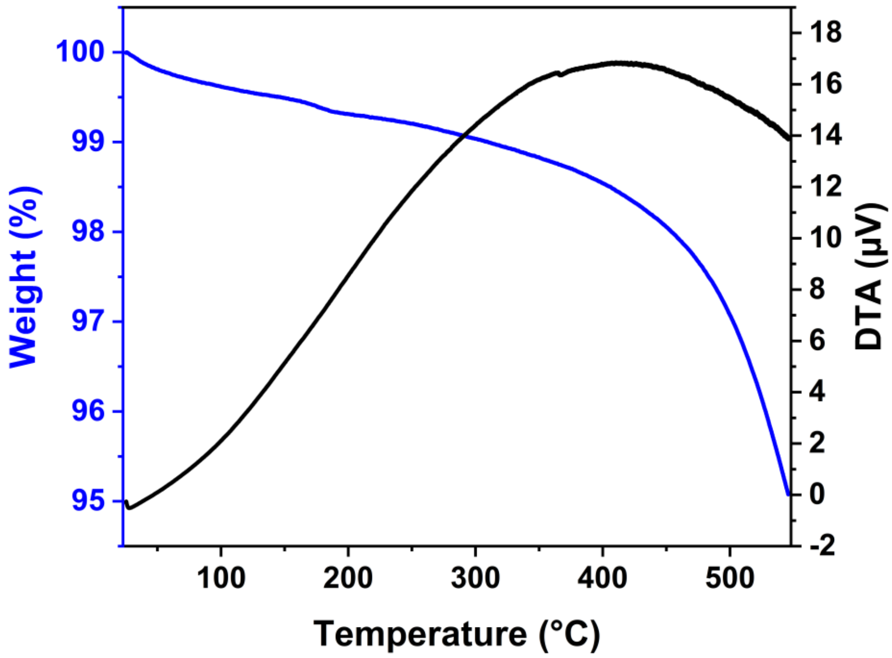

Figure S7: Thermogravimetric analysis (black) and Differential thermal analysis (DTA; red) of the Porous Polymer **PP29**.

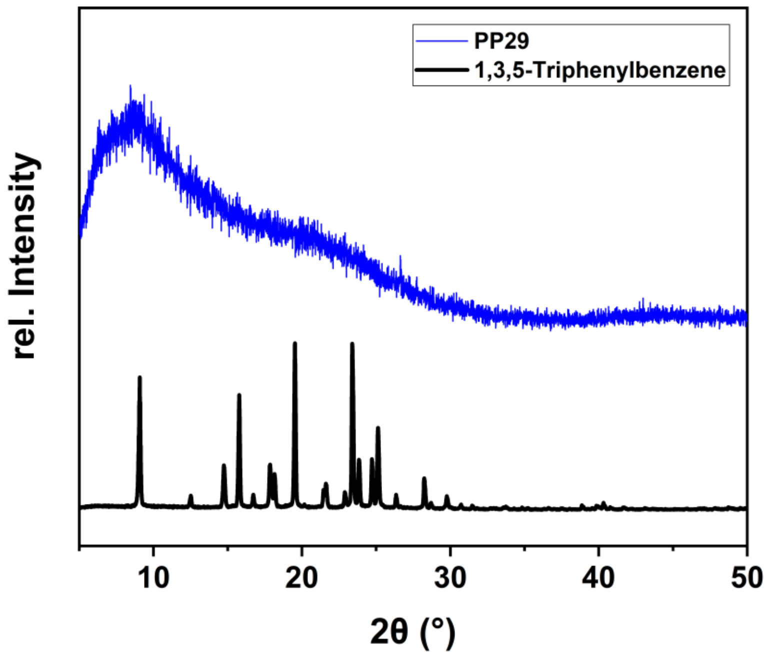

Figure S8: Powder X-ray diffractogram (PXRD) of **PP29** (blue) compared with the monomer 1,3,5-Triphenylbenzene (black), showing the amorphous behaviour of the polymer.

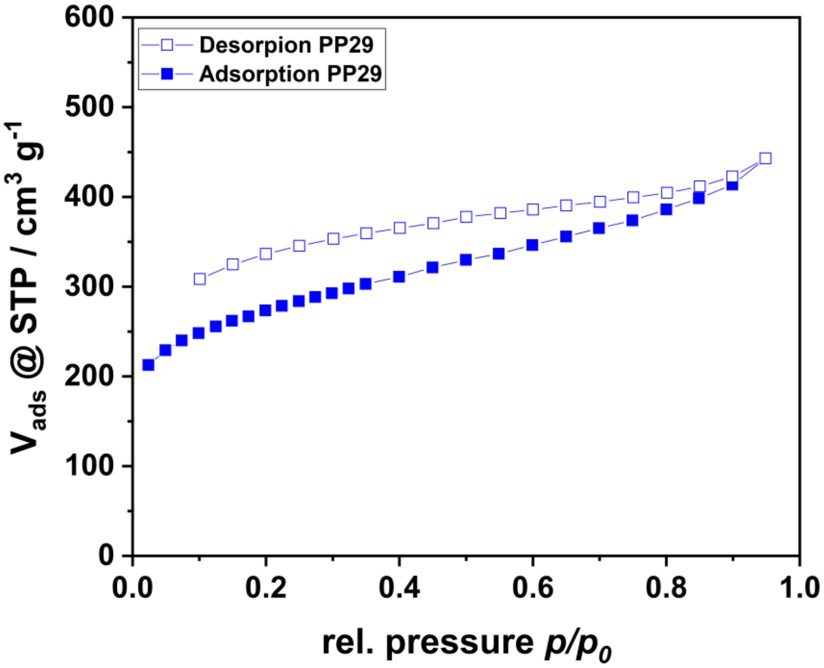

Figure S9: Nitrogen physisorption isotherm IUPAC type I of the porous polymer **PP29** exhibiting a polymer-like swelling behaviour.

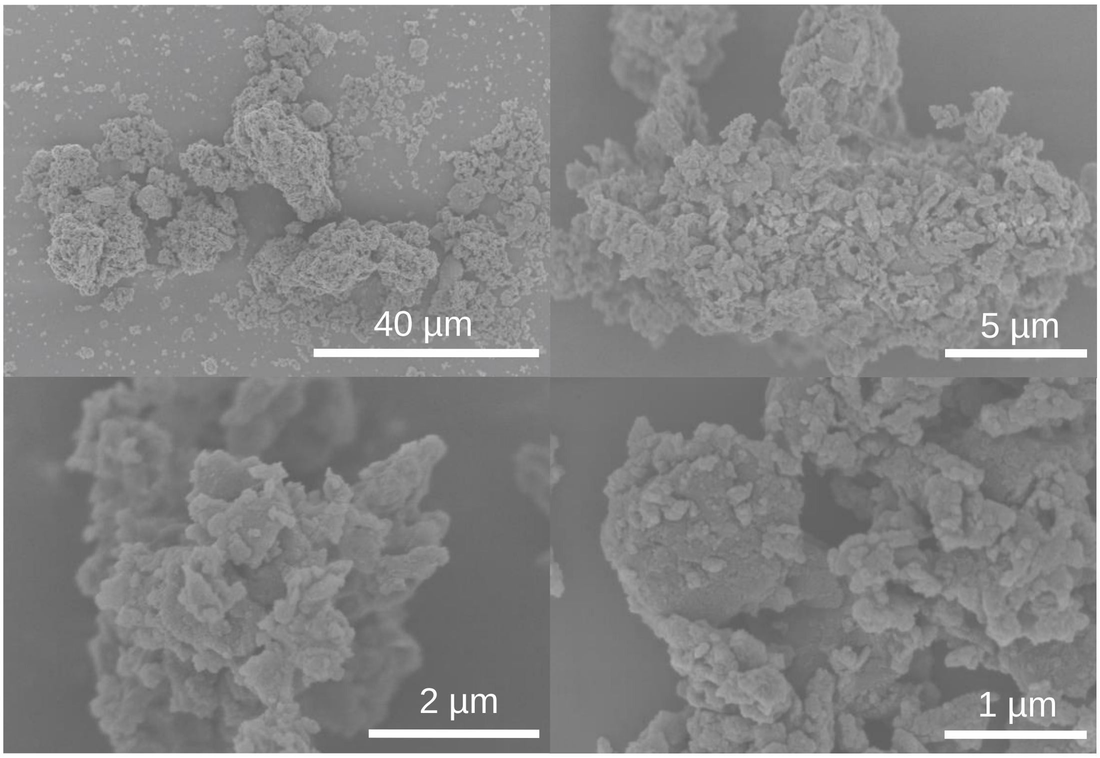

Figure S10: SEM image of the sample **PP29** with a magnitude of 2000 (top, left), of 10000 (top, right), of 30000 (bottom, left) and of 50000 (bottom, right).

3.3. Gas pressure and temperature measurements for LAG

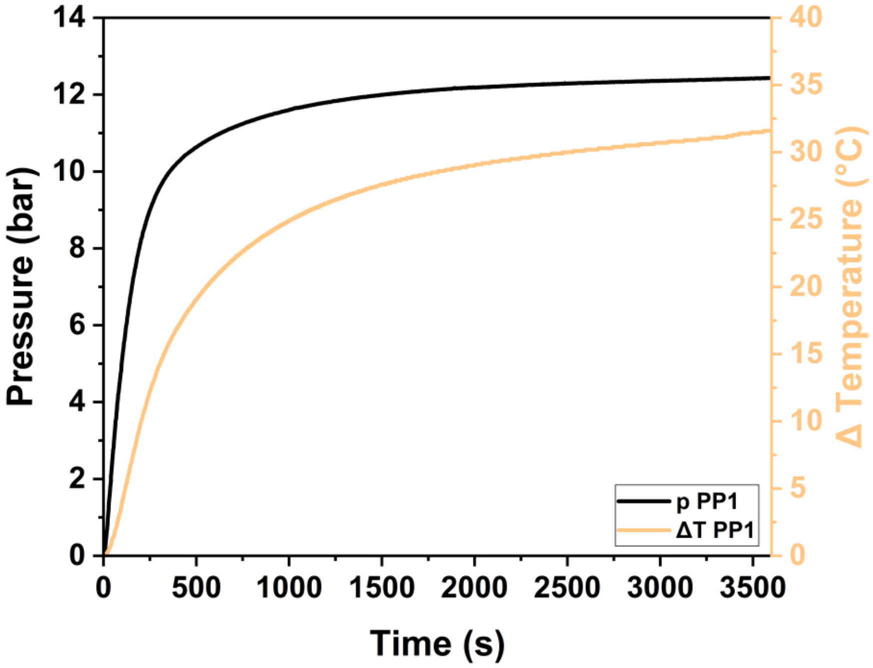

Figure S11: Gas pressure (black) and temperature (beige) measurement for the elongated milling of **PP1**.

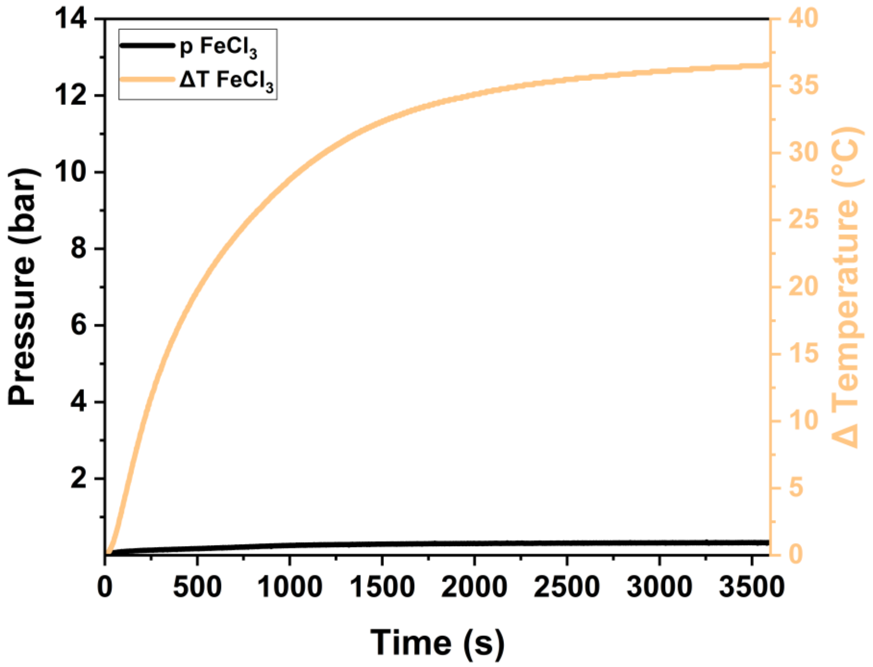

Figure S12: Gas pressure (black) and temperature (beige) measurement for the milling of pure $FeCl_3$.

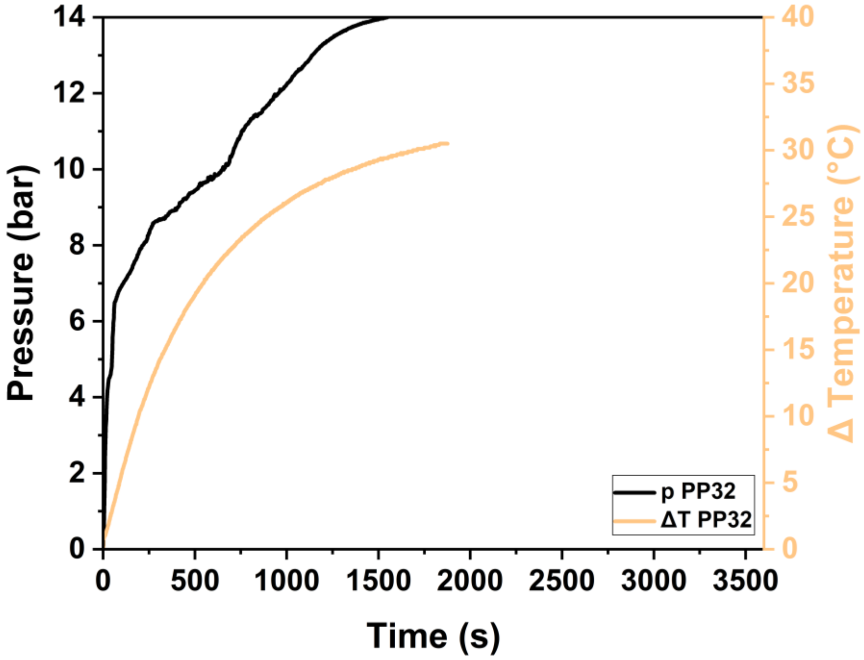

Figure S13: Gas pressure (black) and temperature (beige) measurement for the LAG with 1 ml DCM. A pressure limit of 14 bar was surpassed after ~ 1500 s, which led to milling abortion.

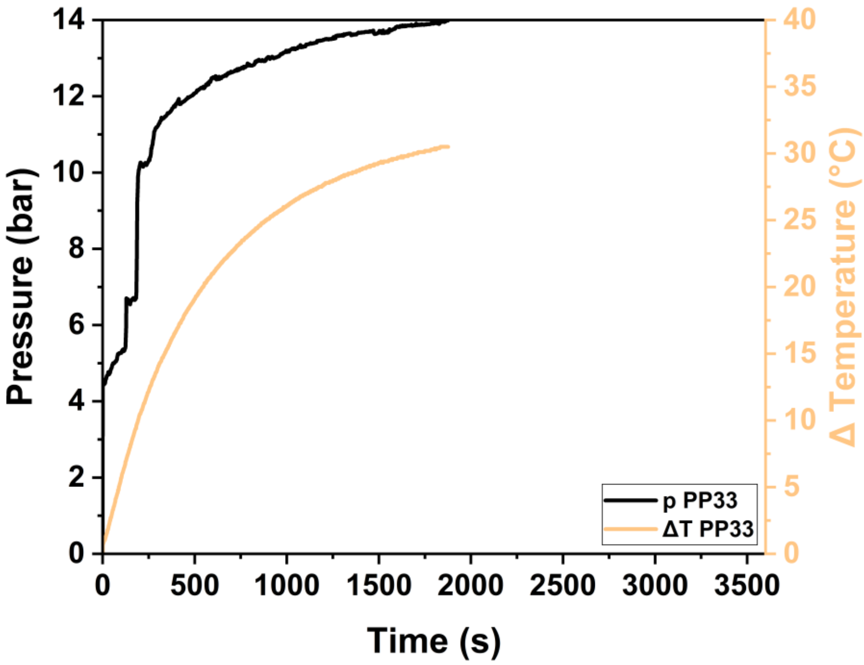

Figure S14: Gas pressure (black) and temperature (beige) measurement for the LAG with 1 ml $CHCl_3$. A pressure limit of 14 bar was surpassed after ~ 2000 s, which led to milling abortion.

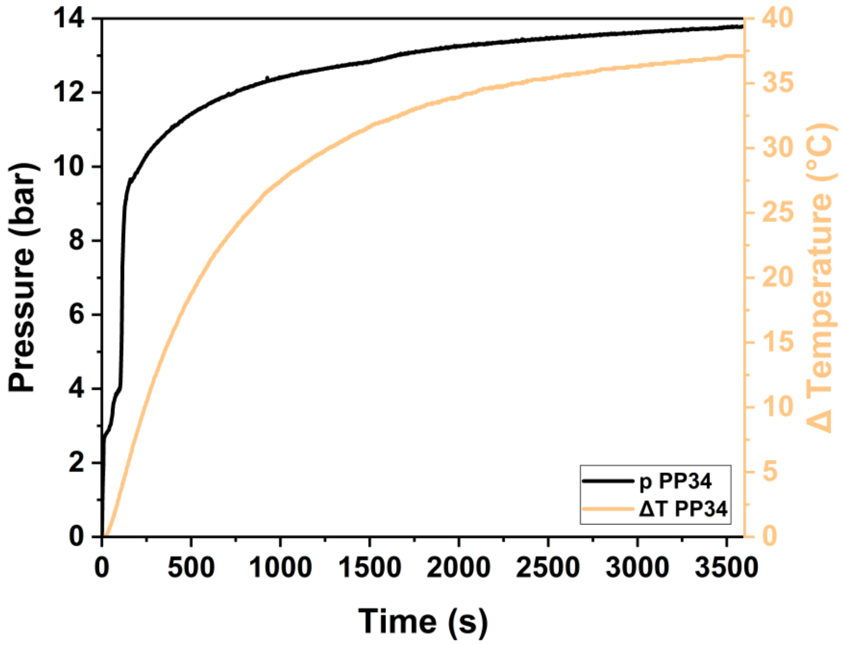

Figure S15: Gas pressure (black) and temperature (beige) measurement for the LAG with 1 ml CH_2Br_2.

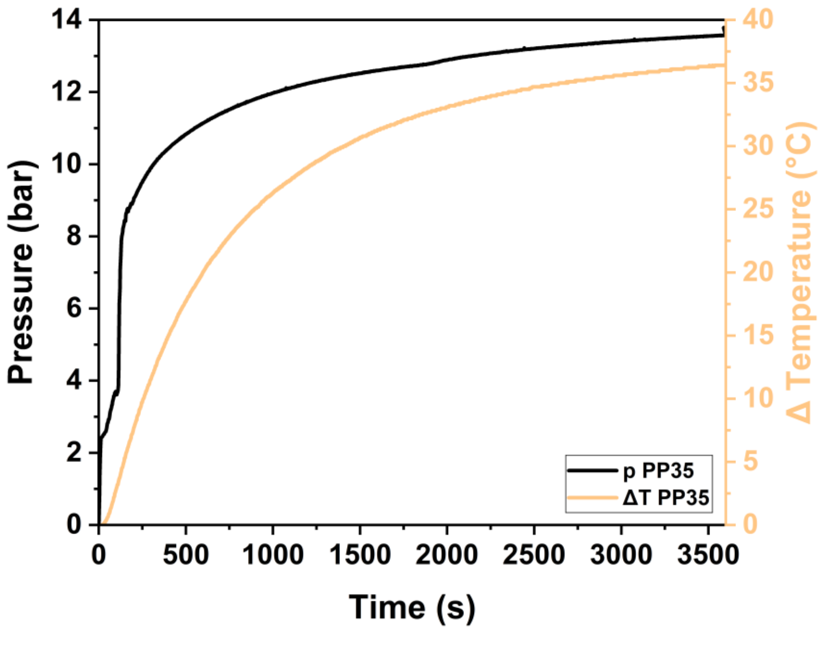

Figure S16: Gas pressure (black) and temperature (beige) measurement for the LAG with 1 ml CH_2BrCl.

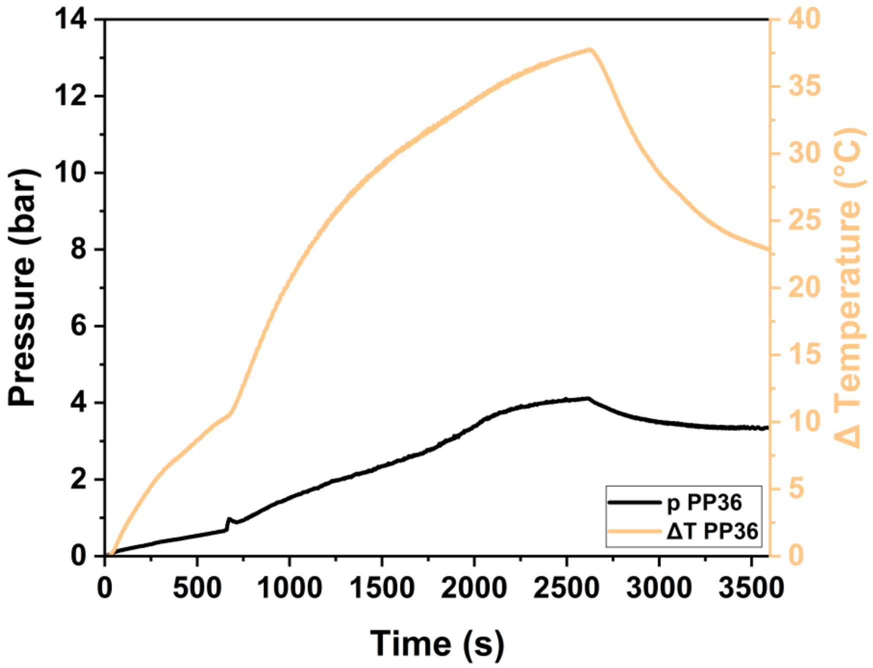

Figure S17: Gas pressure (black) and temperature (beige) measurement for the LAG with 1 ml Et_2O.

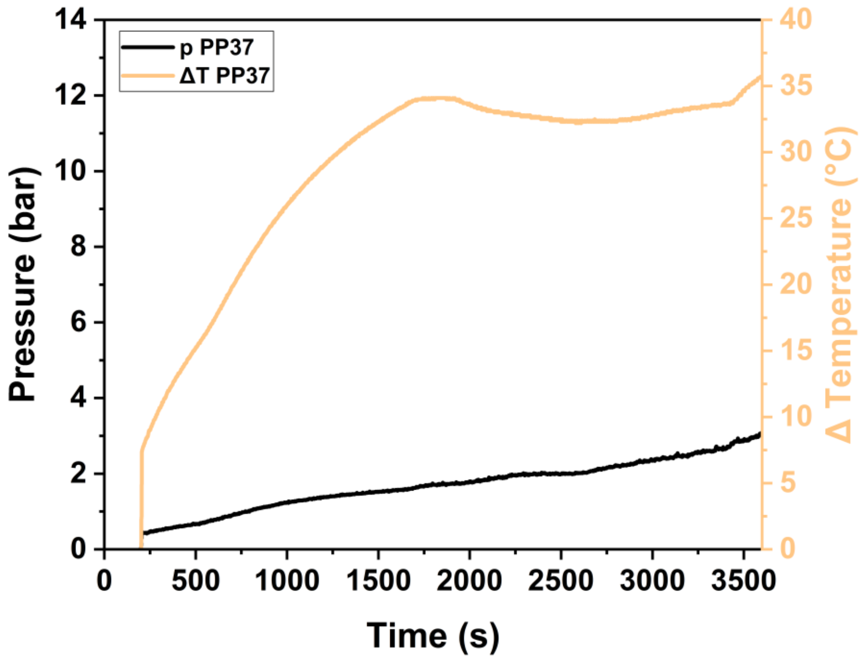

Figure S18: Gas pressure (black) and temperature (beige) measurement for the LAG with 1 ml EtOH.

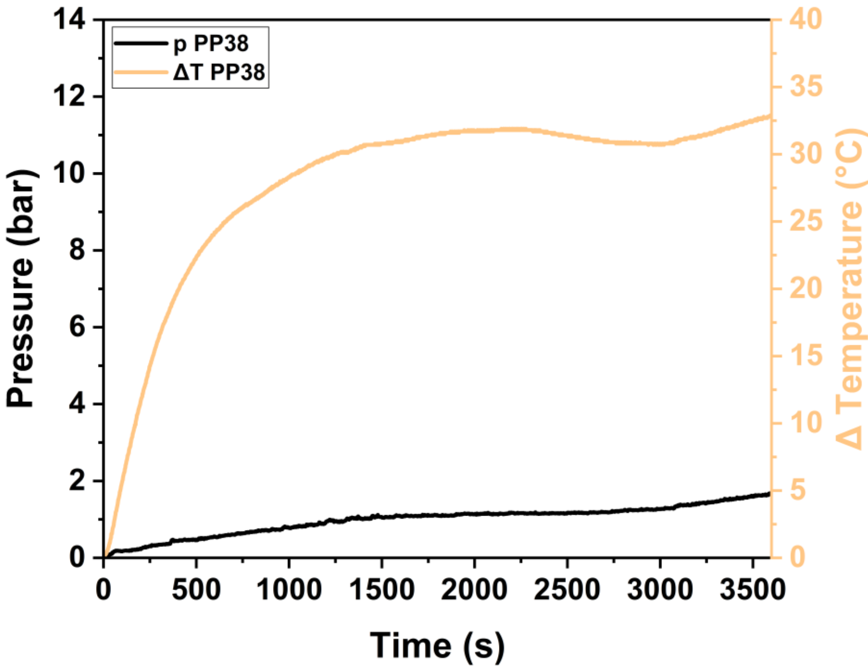

Figure S19: Gas pressure (black) and temperature (beige) measurement for the LAG with 1 ml EtOAc.

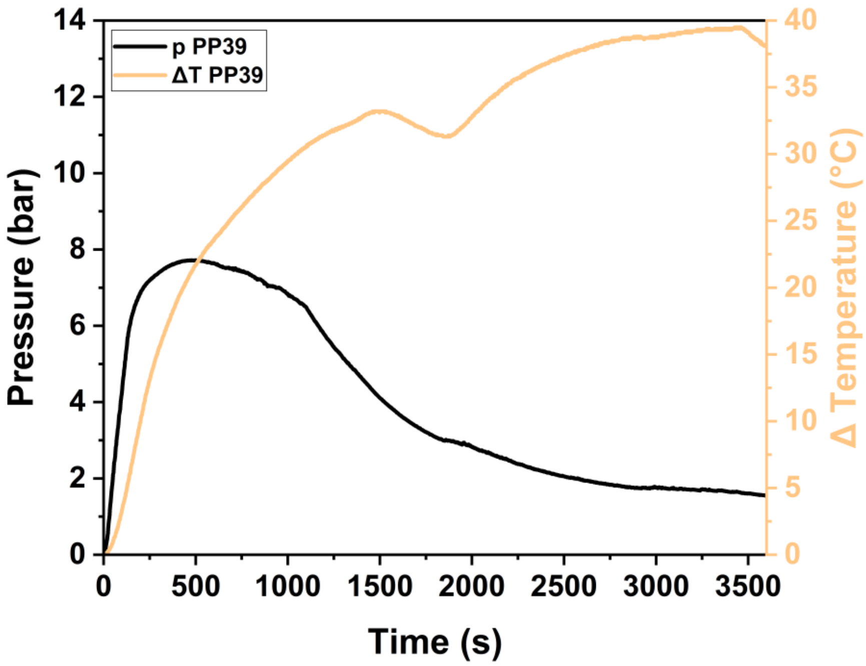

Figure S20: Gas pressure (black) and temperature (beige) measurement for the LAG with 1 ml MeCN.

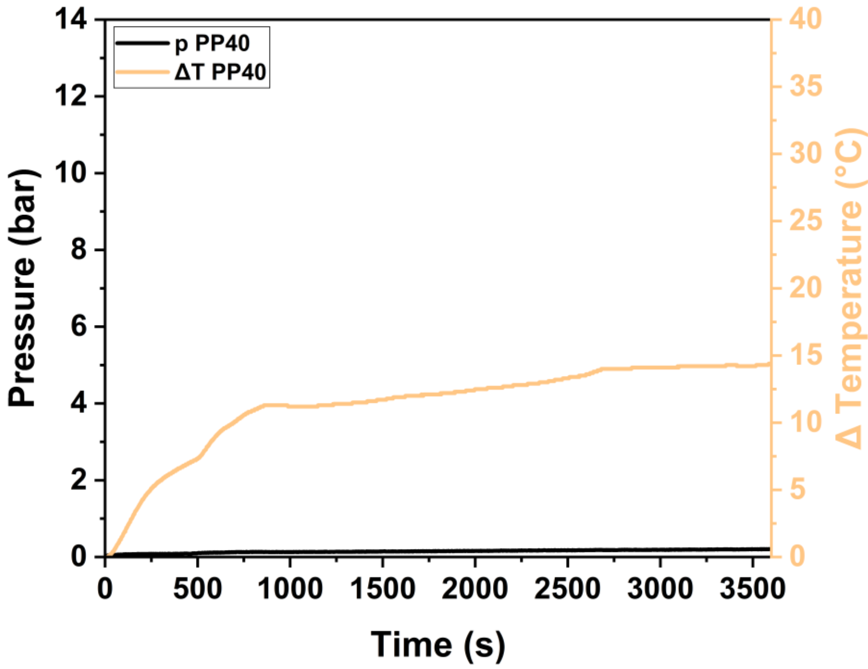

Figure S21: Gas pressure (black) and temperature (beige) measurement for the LAG with 1 ml MeOH. Due to the low temperature increase the reaction was repeated, yielding the same result.

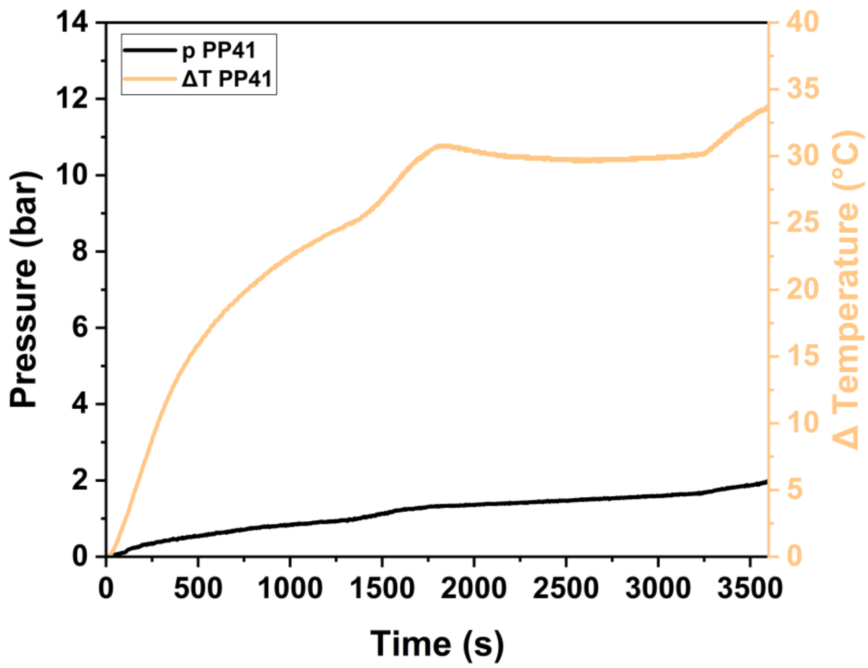

Figure S22: Gas pressure (black) and temperature (beige) measurement for the LAG with 1 ml acetone.

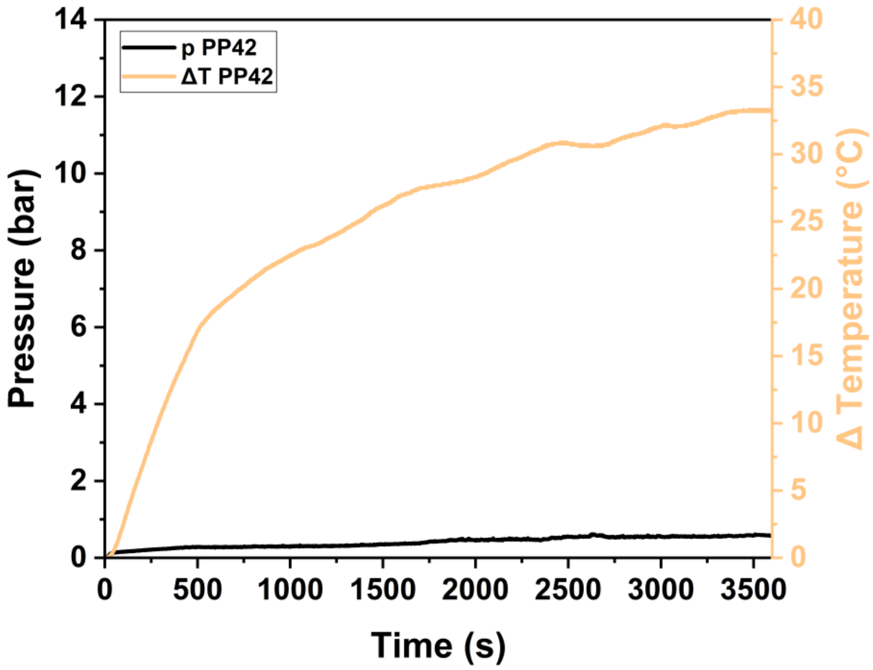

Figure S23: Gas pressure (black) and temperature (beige) measurement for the LAG with 1 ml THF.